'Chromosomal Rainbows' Detect Oncogenic Rearrangements of Signaling Molecules in Thyroid Tumors

Benjamin O'Brien[*,1,2,3], Gregg H. Jossart[1,4,6], Yuko Ito[1,7], Karin M. Greulich-Bode[1,8], Jingly F. Weier[1,5], Santiago Munne[9], Orlo H. Clark[4] and Heinz-Ulrich G. Weier[1]

[1]*Life Sciences Division, E.O. Lawrence Berkeley National Laboratory, Berkeley, CA 94720, USA*

[2]*Department of Cardiothoracic Anaesthesia and Intensive Care, Imperial College Healthcare NHS Trust, Hammersmith Hospital, London, UK*

[3]*Department of Anesthesiology, German Heart Institute, Berlin, Germany*

[4]*Department of Surgery University of California, San Francisco, CA 94115, USA*

[5]*Clinical Laboratories, University of California, San Francisco, CA 94107, USA*

[6]*Laparoscopic Associates of San Francisco, San Francisco, CA 94115, USA*

[7]*National Institute of Science and Technology Policy (NISTEP), Ministry of Education, Culture, Sports, Science and Technology, Tokyo 100-0005, Japan*

[8]*Division Genetics of Skin Carcinogenesis, German Cancer Research Center (DKFZ), Heidelberg, D-69120, Germany*

[9]*Reprogenetics, LLC, Livingston, NJ 07039, USA*

Abstract: Altered signal transduction can be considered a hallmark of many solid tumors. In thyroid cancers the receptor tyrosine kinase (rtk) genes *NTRK1* (Online Mendelian Inheritance in Man = OMIM *191315, also known as '*TRKA*'), *RET* ('Rearranged during Transfection protooncogene', OMIM *164761) and *MET* (OMIM *164860) have been reported as activated, rearranged or overexpressed. In many cases, a combination of cytogenetic and molecular techniques allows elucidation of cellular changes that initiate tumor development and progression. While the mechanisms leading to overexpression of the rtk *MET* gene remain largely unknown, a variety of chromosomal rearrangements of the *RET* or *NTKR1* gene could be demonstrated in thyroid cancer. Abnormal expressions in these tumors seem to follow a similar pattern: the rearrangement translocates the 3'- end of the rtk gene including the entire catalytic domain to an expressed gene leading to a chimeric RNA and protein with kinase activity. Our research was prompted by an increasing number of reports describing translocations involving ret and previously unknown translocation partners.

We developed a high resolution technique based on fluorescence *in situ* hybridization (FISH) to allow rapid screening for cytogenetic rearrangements which complements conventional chromosome banding analysis. Our technique applies simultaneous hybridization of numerous probes labeled with different reporter molecules which are distributed along the target chromosome allowing the detection of cytogenetic changes at near megabasepair (Mbp) resolution. Here, we report our results using a probe set specific for human chromosome 10, which is altered in a significant portion of human thyroid cancers (TC's). While rendering accurate information about the cytogenetic location of rearranged elements, our multi-locus, multi-color analysis was developed primarily to overcome limitations of whole chromosome painting (WCP) and chromosome banding techniques for fine mapping of breakpoints in papillary thyroid cancer (PTC).

Keywords: Receptors, cellular signaling, tumors, genes, human chromosomes, rearrangements, molecular cytogenetics, DNA probes.

INTRODUCTION

The transformation of normal human to neoplastic cells is often accompanied by visible cytogenetic alterations, i.e., chromosomal rearrangements such as translocations, deletions or gene amplifications, leading to the deletion or loss of function of tumor suppressing genes or activation of tumor promoting genes. Abnormal signal transduction secondary to activation of proto-oncogenes by fusion to expressed heterologous genes is a common mechanism of malignant transformation in solid tumors [1].

Increasingly, structural chromosome aberrations are found to be pathognomonic for certain solid tumors.

In PTC [2], it has been reported that activation of rtk genes such as *RET* or neurotrophic receptor kinase type I (*NTRK1*) by intra- or interchromosomal rearrangements causes altered signal transduction and ultimately malignant

*Address correspondence to this author at the Department of Cardiothoracic Anaesthesia and Intensive Care, Imperial College Healthcare NHS Trust, Hammersmith Hospital, London W12 0HS, UK; Tel: +44-2033133991; Fax: +44-2033135373; E-mail: benobrien@doctors.org.uk

1876-3901/10

transformation of the cells [3-9]. Since the key events in neoplastic transformation are expected to be among the most commonly found alterations in phenotypically related tumors, the localization of chromosomal breakpoints is an important step towards positional cloning of the disease causing gene(s). Towards this end, numerous techniques have been developed, several of which depend on enumeration and localization of specific DNA sequences *in situ*.

Chromosome banding techniques require high quality metaphases that are often difficult to obtain from tumor cells. Additionally, the ability to detect subtle rearrangements depends not only on the quality of the metaphase spreads but also on the experience of the cytogeneticist performing the study. The development of FISH with whole chromosome painting (WCP) probes was a major advancement over classical cytogenetic banding techniques [10, 11]. Screening for translocations involving non-homologous chromosomes by multi-color WCP has proven very useful [12-15]. Nevertheless, WCP probes are unsuitable to detect most intrachromosomal rearrangements and small deletions [1, 16].

Physically mapped large insert DNA clones and access to recombinant DNA libraries representing many equivalents of the human genome now allow the development of molecular cytogenetic procedures that complement conventional cytogenetic analysis techniques, i.e., chromosome banding, and will eventually lead to an accelerated identification of disease genes. Furthermore, advances in computer-assisted multi-color fluorescence microscopy have aided the development of high resolution, artificial color banding patterns for each human chromosome based on hybridization of specifically coded DNA probes. This strategy has been suggested earlier and the pioneering work of several groups deserves appropriate credit.

Lichter and coworkers [17] demonstrated how data from genetic and physical maps of chromosome 10 can be linked by *in situ* hybridization on to metaphase chromosome spreads and that selecting clones in adequately large intervals ensures consistent probe order in FISH experiments. Concurrently, Lengauer, *et al*. proposed the generation of what they called "Chromosomal Bar Codes" by combining WCP's with locus-specific probes derived from yeast artificial chromosome (YAC) clones. Although their contribution to the field was significant, the actual resolution of their 'barcodes' suffered from having only relatively few probes spread over 24 different chromosome types and a limitation to only two haptens and, thus, two probe fluorescence colors [11]. Combinatorial probe labeling [18-20] with three independent fluorescence wavelength intervals for probe detection allows one to significantly increase the density of probes that can be hybridized simultaneously along the target chromosome thereby approaching the high resolution of banding techniques. Liehr, *et al*. described 'Multicolor Chromosomal Banding' utilizing combination of YAC/BAC probes and region-specific microdissection DNA libraries for chromosomes 2, 13, and 22, which yields a resolution in the order 4-10 clones per chromosome band or roughly 2-3 million base pairs (Mbp) [21]. More recently, Lu, *et al*. described 'DNA probe pooling' as a way to improve hybridization efficiency and speed [22] emphasizing the fact that larger FISH targets lead to consistently higher FISH success.

Our main interest in developing the technique described here stems from our ongoing investigations of genetic alterations in human thyroid carcinomas. In these tumors, certain chromosomes (1, 2, 3, 10, 11, 17, and 19) appear to be more frequently rearranged than others [23-29] prompting us to develop probe sets which bind specifically to selected sites along these chromosomes. To obtain the power necessary to detect small deletions and rearrangements reported for thyroid carcinomas [3, 30-32], we chose probes which map along the target chromosome(s) in intervals of roughly 0.06 units of its fractional length [17]. For a C-group chromosome such as chromosome 10 with an estimated size of ~140 Mbp, this number translates to approximately 8 Mbp between hybridization probes. Thus, for covering chromosome 10 with a multicolor 'chromosomal rainbow' set (CR10) we selected 16 clones from the Dupont P1 and the CEPH/Genethon yeast artificial chromosome (YAC) libraries [33, 34]. In this article, we describe the selection of the 12 P1 and four YAC clones, and the evaluation and application of CR10. After optimization using normal metaphase spreads, the chromosomal rainbow technique was applied to metaphase spreads of the cell line TPC-1 established from a papillary variant of TC [30]. As reported earlier, this cell line carries a complex t(1;10;21) translocation, a *RET*-activating *RET*/*PTC1* rearrangement and a deletion involving the locus D10S170 [8, 32, 35, 36] (Fig. **1A**). We furthermore applied the CR10 set in two typical applications: characterization of a marker chromosome in the follicular TC cell line FTC-236, derived from a pulmonary metastases, and for breakpoint mapping in the case of a balanced reciprocal translocation t(4;10) in a patient enrolled in an *in vitro* fertilization (IVF) program (Fig. **1B**) [21, 37, 38].

MATERIALS AND METHODS

Cells and Metaphase Spreads

Metaphase spreads were prepared from established cell lines and PHA stimulated short term lymphocyte cultures using standard techniques of colcemid block, hypotonic treatment with 75 mM KCl and fixation in acetic acid:methanol (1:3, vol.: vol.) [21]. Metaphase spreads of the thyroid cancer cell lines TPC-1 and FTC-236 were prepared from cells grown on slides [39]. Slides were stored at -20°C under nitrogen in sealed plastic bags. Prior to hybridization, cells on slides underwent digestion with RNAse A (Roche Molecular Systems, Indianapolis, IN) (1 mg/ml at 37°C for 1 hour) and blocking with gelatin (0.05% in water, weight:vol.) (Sigma, St. Louis, MO) [40].

Probe DNA Preparation and Labeling

The P1 DNAs were extracted from overnight cultures following an alkaline lysis protocol [41]. The YAC DNAs were isolated from 48 hour liquid cultures following a standard protocol using yeast lytic enzyme (ICN, Aurora, OH) [42]. The DNAs were quantitated by Hoechst fluorometry using a Hoefer TK 100 instrument (Hoefer, South San Francisco). Probe DNAs were labeled by random priming as described previously [35, 42]. Probes used in the CR10 rainbow set are listed in Table **1**. Our probe labeling

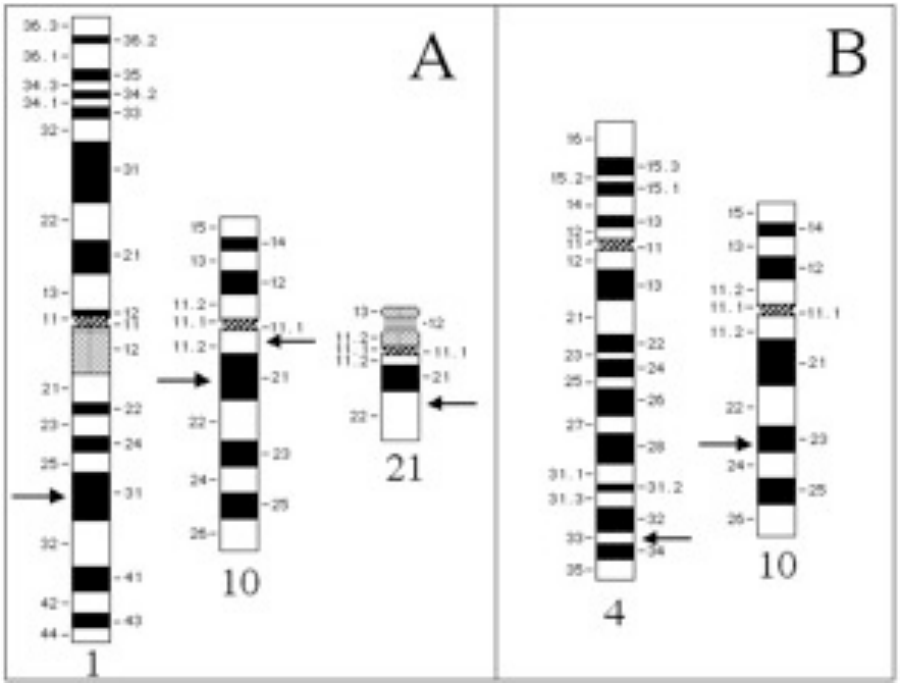

Fig. (1). Chromosome idiograms depicting chromosomes involved in rearrangements. A) Aberrant chromosomes in the papillary thyroid cancer cell line TPC-1 with t(1;10;21) (1pter>1q31::21q22.1>21qter; 10q11.2>10pter::1q31>1qter; 21pter>21q22.1::10q21.2 >10q11.2::10q21.2>10qter). **B**) The approximate locations of the translocation breakpoints in our patient carrying a balanced t(4;10)(q33;q23). Arrows indicate the breakpoints.

and detection scheme is summarized in Table **2**. Yellow fluorescence signals were obtained using probes that had been random primed in the presence of equimolar ratios of digoxigenin-11- (dig) and fluorescein-12-dUTP (fluorescein isothyocyanate, FITC; Roche).

Fluorescence *In Situ* Hybridization

The hybridization mixtures contained 70 µl of human COT-1™ DNA (1 mg/ml, Gibco/LTI), 17 µl of salmon sperm DNA (10 mg/ml; Invitrogen. Carlsbad, CA) and between 60 - 120 ng of each probe, depending on

Table 1. The Probe Set for CR10 Rainbow Hybridization

Location	Fractional Length	Marker	Probe Type	Name	Probe Label	Emission	Display Color
10 p 15	0.017	D10S249	P1	78 E 1	digoxigenin	orange	red
10 p 14	0.097	D10S547	P1	91 A 2	biotin	infrared	purple
10 p 13	0.154	D10S603	P1	81 G 1	FITC	green	green
10 p 12	0.214	D10S588	P1	87 G 10	dig. and FITC	orange and green	yellow
10 p 11.2	0.298	D10S578	P1	98 D 7	digoxigenin	orange	red
10 q 11.2	0.401	ret	P1	58 C 11	biotin	infrared	purple
10 q 21	0.443	D10S539	P1	101 C 7	FITC	green	green
10 q 21	0.478	D10S170	P1	29 F 6	dig. and FITC	orange and green	yellow
10 q 22	0.541	D10S537	P1	106 H 5	digoxigenin	orange	red
10 q 22-23	0.601	D10S607	P1	51 H 2	biotin	infrared	purple
10 q 23	0.671	D10S541	P1	60 D 11	FITC	green	green
10 q 24.1	0.742	NFkB-2	P1	66 E 12	dig. and FITC	orange and green	yellow
10 q 24.3	0.812	D10S597	YAC	911 D 9	digoxigenin	orange	red
10 q 25.2	0.871	D10S	YAC	858 H 7	biotin	infrared	purple
10 q 25-26	0.923	D10S209	YAC	937 A 6	FITC	green	green
10 q 26	0.981	D10S217	YAC	932 F 11	dig. and FITC	orange and green	yellow

Table 2. The FISH Probe Detection Scheme

Label	First Layer	Second Layer	Fluorescence Color
biotin	none	avidin-Cy 5	infrared
digoxigenin	none	rhodamine-labeled sheep-anti-digoxigenin	orange
fluorescein	anti-FITC raised in mice	FITC-labeled goat-anti-mouse	green

hybridization quality and signal intensity of individual probes. The DNA was precipitated in ethanol and resuspended in 3 µl water, before 7 µl of Master Mix 2.1 [42] were added in order to have the probe finally dissolved in 55% formamide (FA; Invitrogen), 10% dextran sulfate and 2xSSC, pH 7.0. The probe mixture was then heat-denatured at 75°C for 7 minutes and preannealed at 37°C for 30 min. Slides were denatured for 3.5 minutes in 70% FA/2x SSC, pH 7.0 at 75°C and dehydrated in a 70%, 85%, 100% ethanol series, two minutes each. About 10 µl of hybridization mixture were placed on the denatured samples, covered with a 22 mm x 22 mm coverslip, sealed with rubber cement and incubated for 42-46 hours at 37°C in a humidity chamber.

Detection

Posthybridization washes were performed as described and included three washes in PN buffer (Na_2HPO_4-7 hydrate/NaH_2PO_4-1 hydrate, pH 8, 0.05% Non-Idet P-40 (Sigma)) [41, 42]. Unspecific binding sites were blocked with PNM (5% nonfat dry milk, 0.1% NaN_3 in PN buffer) [43]. The different layers of fluorochrome-labeled avidin or antibodies were applied in the concentrations listed in Table **3**. The yellow color was generated by overlapping green and red signal, i.e., by hybridization of probes labeled simultaneously with digoxigenin and FITC. After each antibody layer, slides underwent three 10 min. washes in PN with agitation and were again blocked with PNM. After the final wash in PN, slides were washed 10 min. in 0.1% Tween-20 (Sigma) in 2xSSC, mounted with 4,6-diamino-2-phenylindole (DAPI) (0.1µg/ml in (0.1% p-phenylenediamine dihydrochloride (Sigma), 0.1x PBS (Invitrogen), 45 mM $NaHCO_3$, 82% glycerol, pH 8.0) and coverslipped. Images of the *in situ* hybridization results were recorded on a Zeiss Axioskope microscope (Zeiss, Oberkochen, Germany) equipped with a cooled CCD camera (Photometrics CH-250, Phoenix, AZ) as well as triple- and quadruple-color filtersets for multicolor FISH (Chroma Technology, Bellows Falls, VT).

Initially, we had experimented with a triple wavelength bandpass filter set to detect bound probes in red, green and blue. The blue fluorescent signals of probes detected with AMCA-conjugated avidin (Vector, Burlingame, CA), however, were consistently weak, prohibiting DAPI counterstaining of chromosomes. Our four-color filter set allowed specific excitation of DAPI (blue fluorescence) and additional fluorochromes in up to three different wavelength intervals. Bound probes were detected in individual wavelength intervals centered around 520 nm (FITC, green), 600 nm (rhodamine, red) and 690 nm (Cy5, infrared).

The quadruple-color filter set allowed simultaneous counterstaining of the DNA with DAPI, thereby greatly facilitating the task of finding metaphase cells. The image acquisition system used a monochrome CCD camera and a computer controlled filter wheel to select the wavelength of excitation light, and fluorescence images were acquired individually through a multi-bandpass filter set. For display on RGB monitors and in figures contained in this paper, we assigned the color purple to CY5 signals (red excitation) and show the blue fluorescence from DAPI counterstain (UV excitation) in form of a gray-scale image.

RESULTS

Chromosome 10 was chosen to develop the method of staining “chromosomal rainbows” for cytogenetic analysis. On a normal metaphase chromosome 10, our scheme began (from pter to qter) with a probe visualized in red close to the telomeric region of the short arm of chromosome 10, followed proximally by a probe detected in infrared, next a probe seen in green, and then one in yellow. The next probe, detected in red, started a new cycle of colors (Fig. **2A**), creating a pattern of a chromosome-specific 'rainbow'. Probes derived from YAC clones gave stronger signals than probes prepared from P1 clones (Table **1**), which provided

Table 3. The Concentrations of Detection Reagents

Fluorochrome	Manufacturer	Stock Concentration	Working Dilution
Avidin-Cy5	BDS, Pittsburgh, PA	1 mg/ml	1.5:500
AMCA-avidin	Vector, Burlingame, CA	5 mg/ml	1.0:200
Biotinylated goat-anti-avidin	Vector, Burlingame, CA	500 µg/ml	1.0:100
Rhodamine-labeled sheep-anti-digoxigenin	Roche Molecular, Indianapolis, IN	200 µg/ml	1.0:100
Mouse-anti-FITC	DAKO, Carpinteria, CA	430 µg/ml	1.0:200
FITC-labeled goat-anti-mouse	Vector, Burlingame, CA	1.5 mg/ml	1.0:300

further clues for the identification of marker chromosomes (see below).

Applying the technique to our model system of TPC-1 metaphase spreads, all previously described aberrations involving chromosome 10 [32, 36] could be detected. One homologue of chromosome 10 showed a deletion of locus D10S170 (probe 29F6) (Fig. **2B**). The complex translocation involving chromosomes 1, 10 and 21 was detected in all metaphases analyzed (N=12). The breakpoints along

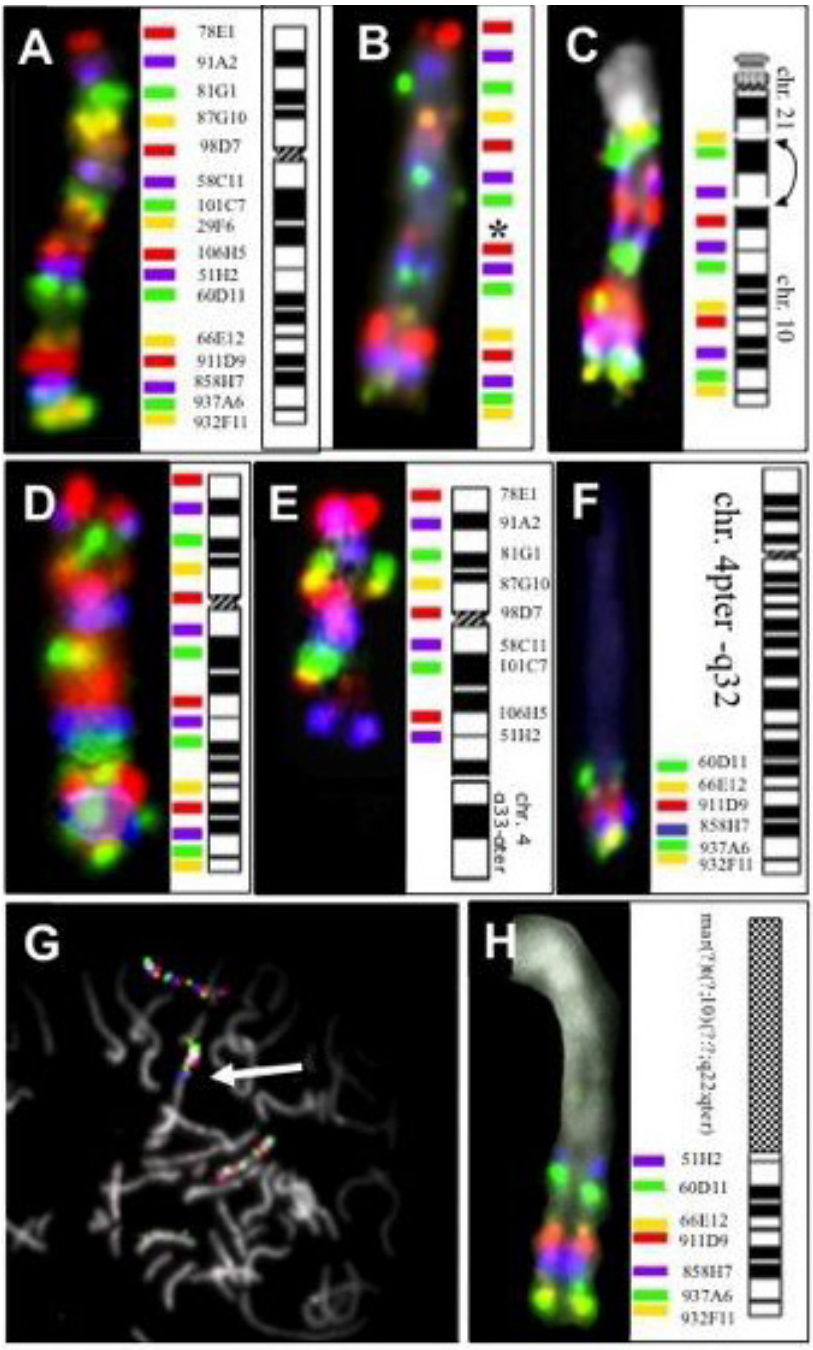

Fig. (2). Hybridization of a chromosomal rainbow set comprised of 16 locus-specific probes that map along chromosome 10. A) In metaphase spreads prepared from short term lymphocyte cultures of a healthy donor, the non-rearranged chromosomes 10 showed all 16 signals of the "chromosome rainbow" in the expected order. **B**) The non-rearranged homologue of chromosome 10 in TPC-1 cells demonstrated the deletion of locus D10S170 (probe 29F6, yellow, indicated by the star). **C**) The der(21) in TPC-1 carried material from the long arm of chromosome 10 from *RET* (probe 58C11, purple) to qter. The arrows indicate the characteristic *RET*-H4/D10S170 (RET/PTC1) inversion. **D**) Metaphase spreads from our patient carrying the reciprocal t(4;10) showed one normal homologue of chromosome 10 when hybridized with a CR10 set lacking the probe for D10S170 (29F6). **E**) A der(10) with a breakpoint distal of probe 51H2. **F**) A der(4) carrying the chromosome 10 material flanked by probes 60D11 and 932F11. **G**, **H**) Cell line FTC-236 showed that metaphase spreads contained 2 normal copies of chromosome 10 and a larger marker chromosome (arrow) that carry chromosome 10 material flanked by probes 51H2 and 932F11. Images in **A-C** were reproduced with kind permission from Springer Verlag, Heidelberg.

chromosome 10, the paracentric inversion and the orientation of the rearranged parts of chromosome 10 could be described easily based on the sequence of colored hybridization signals. The entire p-arm, the centromere and band 10q11 with the breakpoint being distal to probe 58C11, was found reannealed to chromosome 1 fusing to the breakpoint on 1q with its p-terminus in accordance with a previous analysis using a different set of hybridization probes [32]. The remainder of chromosome 10, i.e., part of the long arm, showed a paracentric inversion which was detected by the inverted location of probe 58C11 (purple) and probe 29F6 (yellow) (Fig. **2C**, arrows). Clone 58C11 contained the 3'-end of the ret gene (unpublished). One of the two breakpoints in the paracentric inv(10) (also called 'PTC1') fusing the 3'-end of the proto-oncogene *RET* to the expressed sequence D10S170 maps in intron 11 of the *RET* gene [4, 31], revealing that the entire signal from 58C11 (purple) was translocated.

One single experiment allowed us to map the breakpoint in the case of a reciprocal translocation t(4;10)(q33;q23.2) to the interval flanked by markers D10S507 and D10S541. The rainbow hybridization showed a normal chromosome 10 (Fig. **2D**) in the presence a derivative chromosome 10 with chromosome 4-specific material fused to chromosome 10 distal of D10S607 (probe 51H2, purple) (Fig. **2E**). These hybridizations used only 15 of the 16 probes, and did not include the probe for D10S170 (clone 29F6). The derivative chromosome 4 was found fused to material from the long arm of chromosome 10 distal of D10S541 (probe 60D11, green) (Fig. **2F**). In this case, chromosomal rainbow hybridization indicated neither deletions nor chromosomal inversions.

Using the CR10 rainbow technique, a previously unknown marker chromosome could be identified and described in the follicular thyroid carcinoma cell line FTC-236 [44]. Metaphase spreads showed two apparently normal copies of chromosome 10 in the presence of a marker chromosome, which contained additional chromosome 10 material (Fig. **2G**, arrow). The intensity and sequence of colored signals indicated that this marker carried part of the 10q arm (10q22.3-qter). The breakpoint maps between markers D10S537 (probe 106H5), which is absent from the marker chromosome, and D10S607 (probe 51H2, purple), which was found on this derivative chromosome (Fig. **2H**).

For verification, overexpression of *RET* in TPC-1 cells could rapidly be demonstrated by hybridization of a biotinylated cDNA probe (Fig. **3**). The *RET* specific transcripts (green) reported to be absent in normal thyroid specimens and adenomas [45] were detected in essentially every TPC-1 cell.

DISCUSSION AND CONCLUSION

To facilitate screening of tumor specimens for aberrations involving specific chromosomes, we aimed to develop a technique which enabled us to detect inter- as well as intra-chromosomal rearrangements that were beyond the sensitivity of FISH with WCP probes. The availability of locus-specific probes and novel reporter molecules in combination with advances in optical filter design prompted the development of what we termed 'chromosomal rainbow' hybridization. Multicolor FISH with simultaneous hybridization of chromosome-specific probes had been proposed earlier [11, 20], but as we illustrate through several examples in this paper, a densely hybridizing panel of probes is required to achieve sufficient resolution and sensitivity to detect rearrangements.

In our CR10 probe panel, hybridization quality and efficiency of the probes was consistently high. We incorporated as many P1 clones as possible into the panel since these are generally easier to propagate and more stable than YAC clones [34]. With our spread of probes we could essentially detect any rearrangement involving more than 6-8 Mbp, but would probably miss some of the smaller rearrangements, when they occurred between two probes.

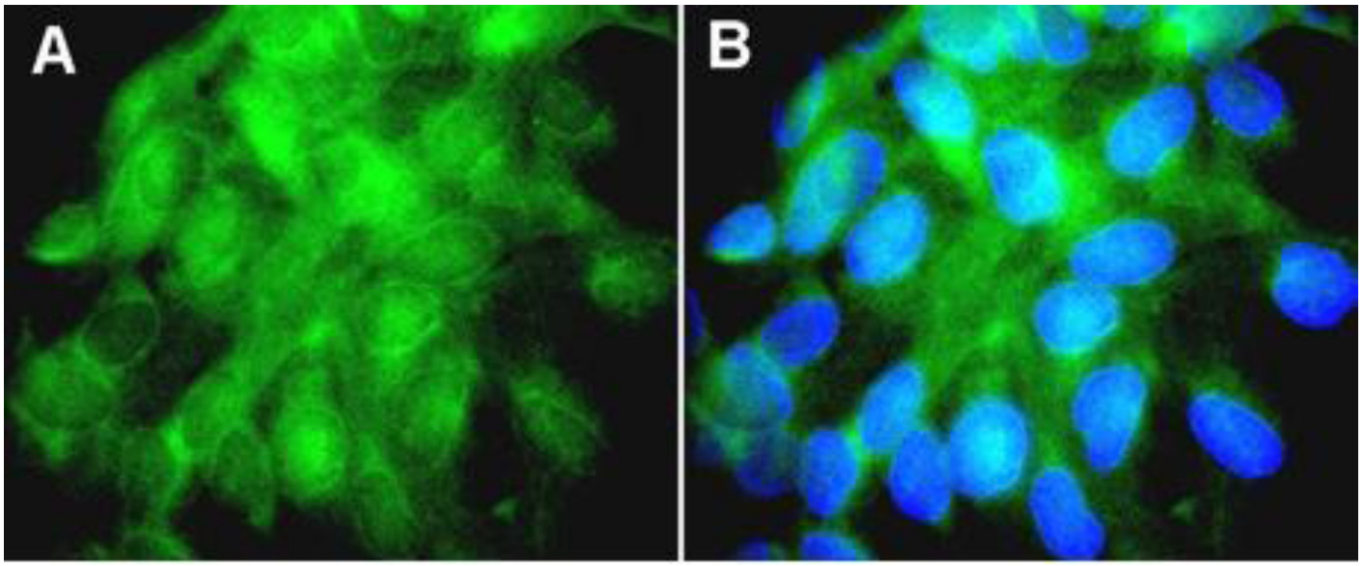

Fig. (3). Hybridization of a *RET* specific cDNA probe reveals high levels of expression in TPC-1 cells. A) Bound biotinylated probe was detected with FITC-conjugated avidin (green). **B**) Nuclear DNA was counterstained with DAPI (blue), and the image was overlayed with the image from **A**).

When small interstitial deletions are suspected, we recommend that the analysis is performed on interphase nuclei, because the chromatin is less condensed so that closely-spaced probes show reduced overlap.

Chromosome 10 was chosen for the establishment of this technique because of its significance in thyroid cancer [5, 8, 23, 31, 46, 47]. Aberrations often involve intrachromosomal rearrangements, e.g., inversions, which cannot be detected by chromosome painting [3, 48]. The use of this chromosome 10-specific probe set, however, will not be limited to thyroid tumors, because rearrangements of chromosome 10 have also been observed frequently in other tumors, such as cancers of the prostate and brain. An increasing number of physically mapped probe collections, such as BAC or YAC libraries [33, 49-51] will facilitate the construction of additional rainbow hybridization panels.

Additional types of DNA probes might be useful and should be considered in such rainbow sets. Deng, *et al*., for example, described the development of chromosome band-specific probes prepared by microdissection, PCR and cloning [52]. This technique was further developed by Guan, *et al*. to the point, where essential coverage of chromosome 6 was achieved by hybridization of 14 subregion-specific probe libraries [53]. While utility of these probes is limited to metaphase chromosome analysis and interphase signals cannot be evaluated, they appear less useful for generating a rainbow hybridization panel due to low resolution. Recently, Liehr, *et al*. demonstrated that a combination of YAC/BAC's and band-specific painting probe prepared by chromosome microdissection can overcome gaps in the BAC/YAC coverage and increase the banding effect [21]. Even more remarkable, Iourov and colleagues extended the use of 'multicolor banding' to the analysis of interphase cell nuclei in cases of mosaic neural aneuploidy [54, 55]. However, concerns relate to probe propagation, distribution and quality control: single clones have no issues with complexity and are easier to maintain, propagate and quality control than high complexity chromosome painting libraries. Furthermore, locus-specific probes can be tailored such that several probes hybridize within the same chromosome band.

The present study focuses solely on rearrangements involving chromosome 10. However, additional susceptibility loci for Familial Non-Medullary Thyroid Cancer (FNMTC) have been recently identified in classic isolated cases of FNMTC (1q21, 6q22, 8p23.1-p22, and 8q24) [47, 56]. Extrapolating our probe spacing to chromosome 6, we would apply 25 probes to cover the entire chromosome 6, whereas Guan, *et al*. reported 14 useful probe libraries derived from the dissection of individual chromosome bands [53]. Using BAC clones, probe coverage can easily be increased to achieve a sub-Mbp resolution, while probe pooling strategies minimize the steps to prepare the FISH probes without sacrificing sensitivity [22, 51, 57, 58].

In its present state of development, rainbow hybridizations allow staining of only one single chromosome for unambiguous mapping of breakpoints and marker chromosome identification. This limitation might be overcome by using additional reporter molecules and/or observation in multiple fluorescence wavelength intervals. Also, more sophisticated equipment such as the spectrofluorometer approach utilized in 'Spectral Karyotyping' or 'Spectral Imaging' [59, 60] might extend the useful range of this promising technique.

Nevertheless, results presented here underline the immediate utility of the 'chromosomal rainbow' technique. The observation of a breakpoint at 10q22-23 in FTC-236, for example, may document a non-random aberration in follicular thyroid carcinomas, similar to studies implicating this region in thyroid adenomas [61]. The breakpoint in our t(4;10) carrier, on the other hand, mapped close to the marker D10S541 which appears to fall in a rather unstable genomic region reported to be rearranged in numerous human tumors such as gliomas, breast and prostate cancer [62, 63]. While the carrier of the balanced translocation showed no disease symptoms other than reproductive problems, it is likely that allelic loss leading to inactivation of tumor suppressor genes in thyroid adenomas [61] may also be found in FTC-236 and related cell lines. Further studies of loss of heterozygosity (LOH) or FISH assays using gene- and locus-specific probes in the interval D10S541-D10S607 (i.e., PTEN or MMCA1 and D10S579, D10S1735, D10S1739, respectively) will help to evaluate possible alterations of these loci in thyroid tumors. We prefer FISH studies with probes densely distributed in the region of interest, since, unlike LOH probes, all FISH probes are informative and allelic loss will become evident immediately by counting the number of hybridization signals for any locus being studied.

In sporadic as well as radiation-induced PTC, ret rearrangements are the most commonly observed abnormality [5, 46], often termed '*RET/PTC* rearrangement'. It is interesting to note that all known translocation partners of the ret locus are genes which are constitutively expressed in thyroid follicular cells. In addition to driving the expression of the chimeric *RET/PTC* oncogene, these partners also provide a dimerization domain essential for ligand-independent activation of the ret tyrosine kinase [46]. As Tong, *et al*. could demonstrate, the leucine zipper-mediated dimerization is essential for the *PTC1* oncogenic activity and tumor formation in mice [7, 64].

Unlike breakpoint-spanning probe contigs described earlier, which are testing only the integrity of the ret locus [32, 36], the novel rainbow hybridization scheme allows simultaneous delineation of intra-chromosomal rearrangements, thus expediting the process of identifying additional, novel *RET/PTC* translocation partners and with it, potential new targets for therapeutic intervention.

Although our examples illustrate the utility of the method to delineate breakpoints on the long arm of chromosome 10, the same set of probes and hybridization protocol can find immediate application in screening for translocations involving the short arm, which harbors a number of tumor-related genes such as the Kruppel-like transcription factor tumor suppressor gene *KLF6* [65] or the *AF10* gene involved in acute T-cell lymphoblastic leukemia [66].

In conclusion, we present here a novel high-resolution FISH based technique that is immediately applicable, as demonstrated by our successful validation experiments, but that will also form the basis for a variety of future developments, variations and refinements in rapid and

specific scanning for inter- and intra-chromosomal rearrangements.

CONFLICT OF INTEREST

The authors declare that they do not have a conflict of interest.

ACKNOWLEDGEMENTS

We thank Drs. T. Tanaka, S. Jhiang and P. Goretzky for supplying cells and cell lines. This work was supported in parts by a grant from the Director, Office of Energy Research, Office of Health and Environmental Research, U.S. Department of Energy, under contract DE-AC02-05CH11231, the Leonard Rosenman Fund, the Medical Research Service of the Veterans Affairs Medical Center, San Francisco, and NIH grants CA80792, HD45736, CA123370 and CA136685 and part of the project 7 of the Research Consortium Tumor Stem Cells funded by the Deutsche Krebshilfe (German Cancer Aid). Ideograms were kindly provided by D. Adler, Ph.D., Dept. of Pathology, Univ. Washington. We acknowledge the support from staff at Reprogenetics providing metaphase spreads and mapping data. Figures 2A-C are reproduced from Zitzelsberger, O'Brien and Weier: Multi-color FISH-based techniques for the detection of inter- and intrachromosomal rearrangements. *Springer Laboratory Manual – FISH Technology,* Edited by Rautenstrauss and Liehr. Springer Verlag, Heidelberg, 2002.

DISCLAIMER

ABBREVIATIONS

AMCA = 7-Amino-4-methylcoumarin-3-acetic acid

BAC = Bacterial artificial chromosome

CR10 = Chromosomal rainbow set for chromosome 10

cDNA = Complementary DNA

CEPH = Centre d'Études du Polymorphisme Humain

DAPI = 4,6-diamino-2-phenylindole

dig = Digoxigenin

FA = Formamide

FISH = Fluorescence *in situ* hybridization

FITC = Fluorescein isothiocyanate

FTC = Follicular thyroid cancer

ivf = *In vitro* fertilization

LOH = Loss of heterozygosity

Mbp = Megabasepair

OMIM = Online mendelian inheritance in man

PFGE = Pulsed field gel electrophoresis

PN = Na_2HPO_4-7 hydrate/NaH_2PO_4-1 hydrate, pH 8, 0.05% Non-Idet P-40

PNM = 5% nonfat dry milk, 0.1% NaN_3 in PN buffer

PTC = Papillary thyroid cancer

rtk = Receptor tyrosine kinase

TC = Thyroid cancer

YAC = Yeast artificial chromosome

REFERENCES

[1] Albertson DG, Collins C, McCormick F, Gray JW. Chromosome aberrations in solid tumors. Nat Genet 2003; 34: 369-76.

[2] Jossart GH, Clark OH. Well-differentiated thyroid cancer. Curr Probl Surg 1994; 31: 933-1012.

[3] Jhiang SM, Mazzaferri EL. The ret/PTC oncogene in papillary thyroid carcinoma. J Lab Clin Med 1994; 123: 331-7.

[4] Smanik PA, Furminger TL, Mazzaferri EL, Jhiang SM. Breakpoint characterization of the ret/PTC oncogene in human papillary thyroid carcinoma. Hum Mol Genet 1995; 4: 2313-8.

[5] Klugbauer S, Lengfelder E, Demidchik EP, Rabes HM. High prevalence of RET rearrangement in thyroid tumors of children from Belarus after the Chernobyl reactor accident. Oncogene 1995; 11: 2459-67.

[6] Beimfohr C, Klugbauer S, Demidchik EP, Lengfelder E, Rabes HM. NTRK1 re-arrangement in papillary thyroid carcinomas of children after the Chernobyl reactor accident. Int J Cancer 1999; 80: 842-7.

[7] Knostman KA, Venkateswaran A, Zimmerman B, Capen CC, Jhiang SM. Creation and characterization of a doxycycline-inducible mouse model of thyroid-targeted RET/PTC1 oncogene and luciferase reporter gene coexpression. Thyroid 2007; 17: 1181-8.

[8] Gandhi M, Dillon LW, Pramanik S, Nikiforov YE, Wang YH. DNA breaks at fragile sites generate oncogenic RET/PTC rearrangements in human thyroid cells. Oncogene 2010; 29: 2272-80.

[9] Weier HU, Kwan J, Lu CM, *et al.* Kinase expression and chromosomal rearrangements in papillary thyroid cancer tissues: investigations at the molecular and microscopic levels. J Physiol Pharmacol 2009; 4: 47-55.

[10] Tkachuk DC, Pinkel D, Kuo WL, Weier HU, Gray JW. Clinical applications of fluorescence *in situ* hybridization. Genet Anal Tech Appl 1991; 8: 67-74.

[11] Lengauer C, Speicher MR, Popp S, *et al.* Chromosomal bar codes produced by multicolor fluorescence *in situ* hybridization with multiple YAC clones and whole chromosome painting probes. Hum Mol Genet 1993; 2: 505-12.

[12] Wlodarska I, Mecucci C, De Wolf-Peeters C, *et al.* "Jumping" translocation of 9q in a case of follicular lymphoma. Cancer Genet Cytogenet 1994; 76: 140-4.

[13] Carter NP. Cytogenetic analysis by chromosome painting. Cytometry 1994; 18: 2-10.

[14] Weier HG, Pinkel D, Gray JW. Whole chromosome complementary probe fluorescence staining. In: Meyers RA, Ed. Molecular biology and biotechnology. New York: VCH 1995; pp. 965-8.

[15] Greulich KM, Kreja L, Heinze B, *et al.* Rapid detection of radiation-induced chromosomal aberrations in lymphocytes and

hematopoietic progenitor cells by mFISH. Mutat Res 2000; 452: 73-81.

[16] Vorsanova SG, Yurov YB, Iourov IY. Human interphase chromosomes: a review of available molecular cytogenetic technologies. Mol Cytogenet 2010; 3: 1.

[17] Lichter JB, Difilippantonio MJ, Pakstis AJ, Goodfellow PJ, Ward DC, Kidd KK. Physical and genetic maps for chromosome 10. Genomics 1993; 16: 320-4.

[18] Nederlof PM, Van der Flier S, Wiegant J, *et al*. Multiple fluorescence *in situ* hybridization. Cytometry 1990; 11: 126-31.

[19] Dauwerse JG, Wiegant J, Raap AK, Breuning MH, Van Ommen GJ. Multiple colors by fluorescence *in situ* hybridization using ratio-labelled DNA probes create a molecular karyotype. Hum Mol Genet 1992; 1: 593-8.

[20] Ried T, Baldini A, Rand TC, Ward DC. Simultaneous visualization of seven different DNA probes by *in situ* hybridization using combinatorial fluorescence and digital imaging microscopy. Proc Natl Acad Sci USA 1992; 89: 1388-92.

[21] Liehr T, Weise A, Heller A, *et al*. Multicolor chromosome banding (MCB) with YAC/BAC-based probes and region-specific microdissection DNA libraries. Cytogenet Genome Res 2002; 97: 43-50.

[22] Lu CM, Kwan J, Baumgartner A, *et al*. DNA probe pooling for rapid delineation of chromosomal breakpoints. J Histochem Cytochem 2009; 57: 587-97.

[23] Pierotti MA, Santoro M, Jenkins RB, *et al*. Characterization of an inversion on the long arm of chromosome 10 juxtaposing D10S170 and RET and creating the oncogenic sequence RET/PTC. Proc Natl Acad Sci USA 1992; 89: 1616-20.

[24] Mulligan LM, Gardner E, Smith BA, Mathew CG, Ponder BA. Genetic events in tumour initiation and progression in multiple endocrine neoplasia type 2. Genes Chromosomes Cancer 1993; 6: 166-77.

[25] Sozzi G, Bongarzone I, Miozzo M, *et al*. A t(10;17) translocation creates the RET/PTC2 chimeric transforming sequence in papillary thyroid carcinoma. Genes Chromosomes Cancer 1994; 9: 244-50.

[26] Zedenius J, Wallin G, Svensson A, *et al*. Allelotyping of follicular thyroid tumors. Hum Genet 1995; 96: 27-32.

[27] Lehmann L, Greulich KM, Zitzelsberger H, *et al*. Cytogenetic and molecular genetic characterization of a chromosome 2 rearrangement in a case of human papillary thyroid carcinoma with radiation history. Cancer Genet Cytogenet 1997; 96: 30-6.

[28] Smida J, Salassidis K, Hieber L, *et al*. Distinct frequency of ret rearrangements in papillary thyroid carcinomas of children and adults from Belarus. Int J Cancer 1999; 80: 32-8.

[29] Salassidis K, Bruch J, Zitzelsberger H, Lengfelder E, Kellerer AM, Bauchinger M. Translocation t(10;14)(q11.2:q22.1) fusing the kinetin to the RET gene creates a novel rearranged form (PTC8) of the RET proto-oncogene in radiation-induced childhood papillary thyroid carcinoma. Cancer Res 2000; 60: 2786-9.

[30] Tanaka J, Ogura T, Sato H, Hatano M. Establishment and biological characterization of an *in vitro* human cytomegalovirus latency model. Virology 1987; 161: 62-72.

[31] Grieco M, Cerrato A, Santoro M, Fusco A, Melillo RM, Vecchio G. Cloning and characterization of H4 (D10S170), a gene involved in RET rearrangements *in vivo*. Oncogene 1994; 9: 2531-5.

[32] Jossart GH, Greulich KM, Siperstein AE, Duh Q, Clark OH, Weier HU. Molecular and cytogenetic characterization of a t(1;10;21) translocation in the human papillary thyroid cancer cell line TPC-1 expressing the ret/H4 chimeric transcript. Surgery 1995; 118: 1018-23.

[33] Cohen D, Chumakov I, Weissenbach J. A first-generation physical map of the human genome. Nature 1993; 366: 698-01.

[34] Shepherd NS, Pfrogner BD, Coulby JN, *et al*. Preparation and screening of an arrayed human genomic library generated with the P1 cloning system. Proc Natl Acad Sci USA 1994; 91: 2629-33.

[35] Jossart GH, O'Brien B, Cheng JF, *et al*. A novel multicolor hybridization scheme applied to localization of a transcribed sequence (D10S170/H4) and deletion mapping in the thyroid cancer cell line TPC-1. Cytogenet Cell Genet 1996; 75: 254-7.

[36] Cinti R, Yin L, Ilc K, *et al*. RET rearrangements in papillary thyroid carcinomas and adenomas detected by interphase FISH. Cytogenet Cell Genet 2000; 88: 56-61.

[37] Munne S, Fung J, Cassel MJ, Marquez C, Weier HU. Preimplantation genetic analysis of translocations: case-specific probes for interphase cell analysis. Hum Genet 1998; 102: 663-74.

[38] Cassel MJ, Munne S, Fung J, Weier HU. Carrier-specific breakpoint-spanning DNA probes: an approach to preimplantation genetic diagnosis in interphase cells. Hum Reprod 1997; 12: 2019-27.

[39] Zitzelsberger H, Lehmann L, Hieber L, *et al*. Cytogenetic changes in radiation-induced tumors of the thyroid. Cancer Res 1999; 59: 135-40.

[40] Lakhotia SC, Sharma A, Mutsuddi M, Tapadia MG. Gelatin as a blocking agent in Southern blot and chromosomal *in situ* hybridizations. Trends Genet 1993; 9: 261.

[41] Weier HU, Rhein AP, Shadravan F, Collins C, Polikoff D. Rapid physical mapping of the human trk protooncogene (NTRK1) to human chromosome 1q21-q22 by P1 clone selection, fluorescence *in situ* hybridization (FISH), and computer-assisted microscopy. Genomics 1995; 26: 390-3.

[42] Weier HU, George CX, Greulich KM, Samuel CE. The interferon-inducible, double-stranded RNA-specific adenosine deaminase gene (DSRAD) maps to human chromosome 1q21.1-21.2. Genomics 1995; 30: 372-5.

[43] Weier HU. DNA fiber mapping techniques for the assembly of high-resolution physical maps. J Histochem Cytochem 2001; 49: 939-48.

[44] Hoelting T, Siperstein AE, Clark OH, Duh QY. Epidermal growth factor enhances proliferation, migration, and invasion of follicular and papillary thyroid cancer *in vitro* and *in vivo*. J Clin Endocrinol Metab 1994; 79: 401-8.

[45] Fabien N, Paulin C, Santoro M, *et al*. Detection of RET oncogene activation in human papillary thyroid carcinomas by *in situ* hybridisation. Br J Cancer 1992; 66: 1094-8.

[46] Nikiforov YE. RET/PTC rearrangement in thyroid tumors. Endocr Pathol 2002; 13: 3-16.

[47] Vriens MR, Schreinemakers JM, Suh I, Guerrero MA, Clark OH. Diagnostic markers and prognostic factors in thyroid cancer. Future Oncol 2009; 5: 1283-93.

[48] Fugazzola L, Pierotti MA, Vigano E, Pacini F, Vorontsova TV, Bongarzone I. Molecular and biochemical analysis of RET/PTC4, a novel oncogenic rearrangement between RET and ELE1 genes, in a post-Chernobyl papillary thyroid cancer. Oncogene 1996; 13: 1093-7.

[49] Kim UJ, Shizuya H, Chen XN, *et al*. Characterization of a human chromosome 22 enriched bacterial artificial chromosome sublibrary. Genet Anal 1995; 12: 73-9.

[50] Korenberg JR, Chen XN, Mitchell S, *et al*. A high-fidelity physical map of human chromosome 21q in yeast artificial chromosomes. Genome Res 1995; 5: 427-43.

[51] Weier HU, Tuton TB, Ito Y, *et al*. Molecular cytogenetic characterization of chromosome 9-derived material in a human thyroid cancer cell line. Cytogenet Genome Res 2006; 114: 284-91.

[52] Deng HX, Yoshiura K, Dirks RW, *et al*. Chromosome-band-specific painting: chromosome *in situ* suppression hybridization using PCR products from a microdissected chromosome band as a probe pool. Hum Genet 1992; 89: 13-7.

[53] Guan XY, Meltzer PS, Burgess AC, Trent JM. Coverage of chromosome 6 by chromosome microdissection: generation of 14 subregion-specific probes. Hum Genet 1995; 95: 637-40.

[54] Yurov YB, Vorsanova SG, Iourov IY. GIN'n'CIN hypothesis of brain aging: deciphering the role of somatic genetic instabilities and neural aneuploidy during ontogeny. Mol Cytogenet 2009; 2: 23.

[55] Iourov IY, Vorsanova SG, Liehr T, Kolotii AD, Yurov YB. Increased chromosome instability dramatically disrupts neural genome integrity and mediates cerebellar degeneration in the ataxia-telangiectasia brain. Hum Mol Genet 2009; 18: 2656-69.

[56] Suh I, Filetti S, Vriens MR, *et al*. Distinct loci on chromosome 1q21 and 6q22 predispose to familial nonmedullary thyroid cancer: a SNP array-based linkage analysis of 38 families. Surgery 2009; 146: 1073-80.

[57] Kwan J, Baumgartner A, Lu CM, *et al*. BAC-FISH assays delineate complex chromosomal rearrangements in a case of post-Chernobyl childhood thyroid cancer. Folia Histochem Cytobiol 2009; 47: 135-42.

[58] Lu CM, Kwan J, Weier JF, *et al*. Rapid mapping of chromosomal breakpoints: from blood to BAC in 20 days. Folia Histochem Cytobiol 2009; 47: 367-75.

[59] Schrock E, du MS, Veldman T, *et al*. Multicolor spectral karyotyping of human chromosomes. Science 1996; 273: 494-7.

[60] Fung J, Weier HU, Goldberg JD, Pedersen RA. Multilocus genetic analysis of single interphase cells by spectral imaging. Hum Genet 2000; 107: 615-22.

[61] Marsh DJ, Zheng Z, Zedenius J, *et al*. Differential loss of heterozygosity in the region of the Cowden locus within 10q22-23 in follicular thyroid adenomas and carcinomas. Cancer Res 1997; 57: 500-3.

[62] Li J, Yen C, Liaw D, *et al*. PTEN, a putative protein tyrosine phosphatase gene mutated in human brain, breast, and prostate cancer. Science 1997; 275: 1943-7.

[63] Steck PA, Pershouse MA, Jasser SA, *et al*. Identification of a candidate tumour suppressor gene, MMAC1, at chromosome 10q23.3 that is mutated in multiple advanced cancers. Nat Genet 1997; 15: 356-62.

[64] Tong Q, Xing S, Jhiang SM. Leucine zipper-mediated dimerization is essential for the PTC1 oncogenic activity. J Biol Chem 1997; 272: 9043-7.

[65] Camacho-Vanegas O, Narla G, Teixeira MS, *et al*. Functional inactivation of the KLF6 tumor suppressor gene by loss of heterozygosity and increased alternative splicing in glioblastoma. Int J Cancer 2007; 121: 1390-5.

[66] Chaplin T, Ayton P, Bernard OA, *et al*. A novel class of zinc finger/leucine zipper genes identified from the molecular cloning of the t(10;11) translocation in acute leukemia. Blood 1995; 85: 1435-41.

Received: May 2, 2010 Revised: August 21, 2010 Accepted: October 22, 2010